Pramana – J. Phys. (2017) 88: 35
DOI 10.1007/s12043-016-1350-3

Filamentation of ultrashort laser pulses of different wavelengths in argon

XIEXING QI and WENBIN LIN*

School of Physical Science and Technology, Southwest Jiaotong University, Chengdu 610031, China
*Corresponding author. E-mail: wl@swjtu.edu.cn

MS received 29 January 2016; revised 5 July 2016; accepted 24 August 2016; published online 17 January 2017

Abstract. We investigate the filaments formed by the ultrashort laser pulses with different wavelengths of 400 nm, 586 nm and 800 nm propagating in argon. Numerical results show that, when the input power or the ratio of the input power to the critical power is given, the pulse with 400 nm wavelength has the largest on-axis intensity, as well as the narrowest filament and the most stable beam radius. These results indicate that the pulse with shorter wavelength is more suitable for the long-range propagation in argon.

Keywords. Filament; femtosecond laser; self-focus.

PACS Nos 42.65.–k; 42.65.Re; 52.38.Hb

1. Introduction

In 1995, Braun *et al* [1] carried out a famous experiment with an intense infrared (IR) femtosecond laser pulse, breaking the previously held belief that the intense ultrashort laser pulses were not suitable for long-range propagation. They found that the femtosecond intense laser pulse not only propagates in air but also forms stable filament. Since then, the potential and alluring application prospects of filament are discovered, e.g. control of a high-voltage discharge, self-written waveguide, probing of the environment and remote sensing [2–8]. Because of the demand of broad applications, a large number of theoretical derivations, experimental verifications and numerical simulations are carried out on the physical mechanism of filament formation [9–21].

Experimental study, as a direct and effective research method, was done in air and special noble gas. In air, there are many types of gases making the propagation of femtosecond laser pulse complicated. But, the noble gas is monoatomic and there is no Raman effect or any other complication such as molecular association and fragmentation [18]. Hence, many researchers choose a noble gas such as argon as the propagating medium [21–25].

In this paper, we adopt incident laser pulses having three different wavelengths to study the filament in argon. The content is organized as follows: Section 2 introduces the nonlinear Schrödinger equation for the femtosecond pulse propagation in air with different wavelengths and the computational algorithm employed in the simulations. In §3, the effects of wavelength on the filament in argon are investigated. The conclusions are summarized in §4.

2. Model and algorithm

Expressed in the reference frame moving at the group velocity, the propagation equations of a laser pulse with a linearly polarized incident electric filed $E(r, t, z)$ along the propagation direction z reads as [12–14]

$$\frac{\partial E}{\partial z} = \frac{i}{2k_0}\left(\frac{\partial^2}{\partial r^2} + \frac{1}{r}\frac{\partial}{\partial r}\right)E - \frac{ik''}{2}\frac{\partial^2 E}{\partial t^2} + \frac{ik_0}{n_0}\Delta n_{\mathrm{Kerr}}E - \frac{ik_0}{2}\frac{\omega^2}{\omega_0^2}E - \frac{\beta^{(K)}}{2}|E|^{2K-2}E, \tag{1}$$

$$\frac{\partial \rho}{\partial t} = \frac{\beta^{(K)}}{K\hbar\omega_0}|E|^{2K}\left(1 - \frac{\rho}{\rho_{at}}\right), \tag{2}$$

where t refers to the retarded time in the reference frame of the pulse ($t \to t - (z/v_{\mathrm{g}})$ with $v_{\mathrm{g}} = (\partial\omega/\partial k)|_{\omega_0}$ corresponding to the group velocity of the carrier envelope). The first two terms on the right-hand side of eq. (1) are the linear effects, accounting for the spatial diffraction and the second-order dispersion. The other

three terms represent Kerr effect, plasma defocussing effect and the multiphoton ionization effect, and these terms are the nonlinear effects. In eq. (1), $k_0 = 2\pi/\lambda$ and $\omega_0 = 2\pi c/\lambda$ are the wave number and the angular frequency of the carrier wave, respectively. k'' is the second-order dispersion coefficient and the plasma frequency $\omega = \sqrt{\rho e^2/m_e\varepsilon_0}$ with e, m_e, ρ being the charge, mass and density of the electron. $\beta^{(K)}$ denotes the nonlinear coefficient for K-photon absorption, where K is the minimal number of photons needed to ionize argon.

The evolution of electron density ρ can be calculated as [14]

$$\frac{\partial\rho}{\partial t} = \frac{\beta^{(K)}}{K\hbar\omega_0}|E|^{2K}\left(1 - \frac{\rho}{\rho_{\mathrm{Ar}}}\right). \tag{3}$$

In eq. (3), $\hbar = h/2\pi$ with h the Planck constant and $\rho_{\mathrm{Ar}} = 2.4 \times 10^{25}$ m^{-3} denotes the density of argon under standard atmosphere pressure.

The input electric field envelope is modelled by a Gaussian profile with input power P_{in} as

$$E(r,\ z,\ t)|_{z=0} = \sqrt{\frac{2P_{\mathrm{in}}}{\pi r_0^2}}\exp\left(-\frac{t^2}{t_0^2}\right)\exp\left(-\frac{r^2}{r_0^2}\right), \tag{4}$$

where $r_0 = 1$ mm and $t_0 = 100$ fs denote the radius and duration of the pulse, respectively.

The model is solved via the split-step Fourier method [26], in which all the linear terms are calculated in the Fourier space over a half-step while the nonlinear terms are calculated in the physical space over a second half-step. To integrate the linear part of eq. (1) along the propagation axis, we adopt the Crank–Nicholson scheme [27], which is more stable than the Euler method [28]. For eq. (3), the fourth-order Runge–Kutta method is employed.

We select laser pulses with 400 nm, 586 nm and 800 nm wavelengths. Their propagating coefficients are summarized in table 1 [25,29].

3. Results and discussion

To investigate the filament formed by the femtosecond laser pulses of different wavelengths in argon accurately, we set the incident power P_{in} as $P_{\mathrm{in}} = 8P_{\mathrm{cr}}$, where $P_{\mathrm{cr}} = 3.77\lambda^2/8\pi n_0 n_2$ is the critical power of self-focussing. Figure 1 presents the evolution of laser on-axis intensity, beam radius (defined as e^{-2} of maximum intensity of the pulse), the on-axis electron density, as well as the ratio of energy within the beam radius to the total energy, with the propagation distance z.

From figure 1a, we can see that when the incident power P_{in} is set as $P_{\mathrm{in}} = 8P_{\mathrm{cr}}$, the shorter the wavelength is, the higher is the on-axis intensity, i.e. the clamped intensity is larger. The clamped intensity for 400 nm is nearly 12×10^{17} W m^{-2}, about twice larger than that for 800 nm. It should be noted that the incident power for 400 nm is less than one sixth of that for 800 nm.

The beam radius is plotted in figure 1b. The propagation length of the self-focussing beam until collapse is defined as collapse distance, denoted by L_{c}, and it can be approximated by the following semiempirical formula [30,31]:

$$L_{\mathrm{c}} = \frac{0.367k_0r_0^2}{2\sqrt{[(P_{\mathrm{in}}/P_{\mathrm{cr}})^{1/2} - 0.0852]^2 - 0.0219}}. \tag{5}$$

From figure 1b, we can see that the collapse distances of these three cases obtained by numerical simulations agree with this formula very well. The filament radius of 400 nm is the narrowest. Moreover, the fluctuation of the filament radius of 400 nm is much less than those of 586 nm and 800 nm. These results indicate that the propagating channel is more stable for shorter wavelengths.

Comparing figure 1c with figure 1a, we can see that the positions where the on-axis intensity of the laser pulse arrives at the maximum (or minimum) usually coincide with those at which the electron density increases (or decrease) sharply. The reason for this is that when the laser pulse intensity exceeds the ionization threshold of argon, a large amount of free electrons will emerge by photoionization to cause plasma

Table 1. Propagating coefficients of laser pulses of three different wavelengths.

λ (nm)	n_2 (m^2 W^{-1})	k''(s^2 m^{-1})	K	$\beta^{(K)}$ (W^{1-K} m^{2K-3})
400	4.9×10^{-23}	4.9×10^{-29}	6	1.95×10^{-88}
586	4.9×10^{-23}	2.6×10^{-29}	8	3.50×10^{-123}
800	3.2×10^{-23}	2.1×10^{-29}	11	3.32×10^{-176}

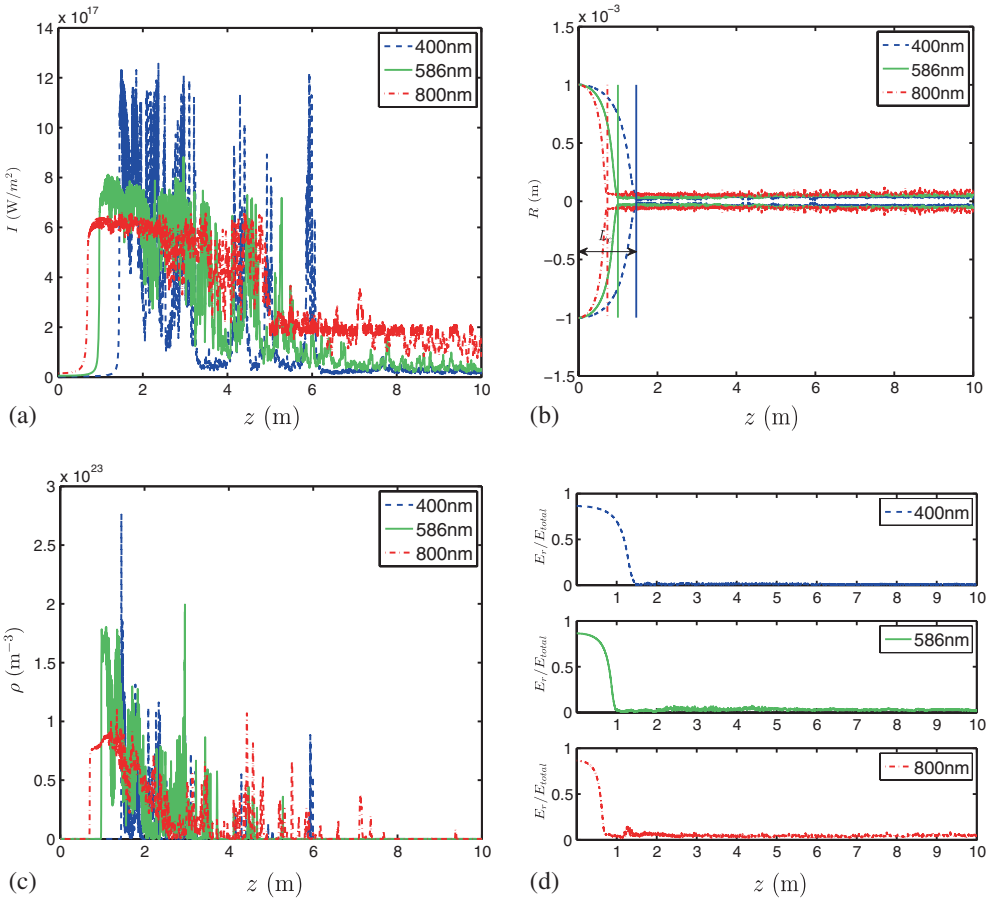

Figure 1. Evolution of the pulse and the on-axis electron density for different wavelengths with the propagation distance z for the same ratio of the incident power to P_{cr}. (**a**) The on-axis intensity of pulse; (**b**) beam radius; (**c**) the on-axis electron density; (**d**) the ratio of energy within the beam radius to the total energy.

defocussing of the laser beam, and this defocussing competes against Kerr focussing until they reach a dynamic balance to form the filament supporting the long distance propagation.

Figure 1d presents the ratio of energy within the beam radius to the total energy along the propagating direction. For 400 nm wavelength, this ratio remains stable after self-focussing. The ratio for 586 nm is similar to that of 400 nm wavelength, but has a little more fluctuation. For 800 nm, this ratio gets the most fluctuation.

In addition, for the beam pulse with shorter wavelength, the length of dispersion is shorter which means the loss due to the dispersion is less, and the ionization potential is lower. The number of K representing the minimal number of photons to ionize argon atom is less so that the energy loss due to the ionization is also less, and the remaining energy can sustain longer distances.

In order to observe the filament more visually, figure 2 plots the light flux along the propagating direction. It can be seen from figure 2 that, the filament is the finest for 400 nm wavelength and get the highest light flux. For 800 nm wavelength, the filament has the widest radius and the lowest light flux.

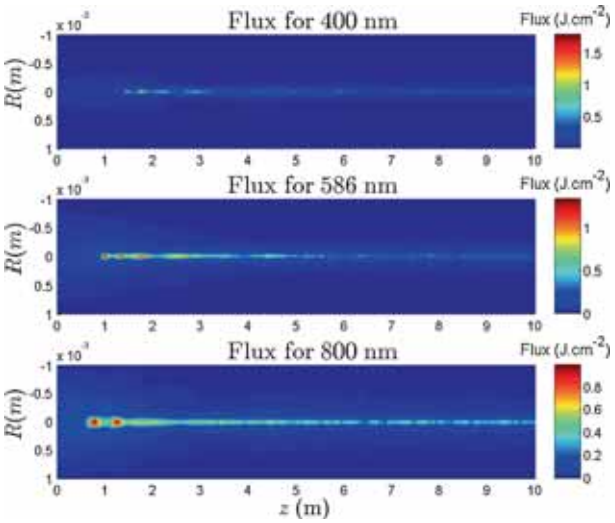

Figure 2. Evolution of the flux of laser pulses with the propagation distance z.

We also simulated the femtosecond filamentation of these different wavelengths for $P_{in} = 6P_{cr}$, $P_{in} = 4P_{cr}$ and $P_{in} = 2P_{cr}$. The conclusions are identical to those above and the results will not be plotted.

For the given incident power P_{in}, the ratio of P_{in} to P_{cr} increases when the wavelength decreases. Considering the single filament like the above simulations, the larger the ratio is, the more obvious the filament becomes. So, we shall not show these simulation results here.

4. Conclusions

We investigated the filamentation of the femtosecond laser pulse for 400 nm, 586 nm, 800 nm wavelengths in argon by numerical simulations. We found that the on-axis intensity and the beam radius become higher and narrower when the wavelength decreases. Moreover, the ratio of the energy within the beam radius to the total energy for 400 nm wavelength is the most stable, implying that the pulse with shorter wavelength is more suitable for the long-range propagation in argon.

Acknowledgements

The authors thank the reviewer for the constructive comments and suggestions for improving the quality of this paper. This work was supported by the Ph.D. Programs Foundation of Ministry of Education of China (No. 20110184110016) and the National Basic Research Program of China (973 Program) Grant No. 2013CB328904, as well as the Fundamental Research Funds for the Central Universities.

References

[1] A Braun, G Korn, X Liu, D Du, J Squier and G Mourou, *Opt. Lett.* **20(1)**, 73 (1965)
[2] M Rodriguez, R Sauerbrey, H Wille, L Wöste, T Fujii, Y B André, A Mysyrowicz, L Klingbeil, K Rethmeier, W Kalkner, J Kasparian, E Salmon, J Yu and J P Wolf, *Opt. Lett.* **27**, 772 (2002)
[3] S Tzortzakis, B Prade, M Franco, A Mysyrowicz, S Huller and P Mora, *Phys. Rev. E* **64**, 057401 (2001)
[4] J J Ju, J S Liu, C Wang, H Y Sun, W T Wang, X C Ge, C Li, S L Chin, R X Li and Z Z Xu, *Opt. Lett.* **37**, 1214 (2012)
[5] S Henin, Y Petit, P Rohwetter, K Stelmaszczyk, Z Q Hao, W M Nakaema, A Vogel, T Pohl, F Schneider, J Kasparian, K Weber, L Wöste and J P Wolf, *Nature Commun.* **l**, 456 (2011)
[6] R Bourayou, G Méjean, J Kasparian, M Rodriguez, E Salmon, J Yu, H Lehmann, B Stecklum, U Laux, J Eislöffel, A Scholz, A P Hatzes, R Sauerbrey, L Woste and J P Wolf, *J. Opt. Soc. Am. B* **22**, 369 (2005)
[7] C P Jisha, V C Kishore, B M John, V C Kuriakose, K Porsezian and C S Kartha, *Appl. Opt.* **47**, 6502 (2008)
[8] V P Kandidov, O G Kosareval, I S Golubtsov, W Liu, A Becker, N Akozbek, C M Bowden and S L Chin, *Appl. Phys. B* **77**, 149 (2003)
[9] X X Qi, C L Ma and W B Lin, *Opt. Commun.* **358**, 126 (2016)
[10] L Wang, C L Ma, X X Qi and Wenbin Lin, *Eur. Phys. J. D* **69**, 72 (2015)
[11] L F Dong, X C Xue, Z Q Yin, S F Qian, J T Ouyang and L Wang, *Chin. Phys. Lett.* **18(10)**, 1380 (2001)
[12] A Couairon and A Mysyrowicz, *Phys. Rep.* **441**, 47 (2007)
[13] H T Wang, C Y Fan, P F Zhang, C H Qiao, J H Zhang and H M Ma, *Opt. Express* **18**, 24301 (2010)
[14] P Béjot, C Bonnet, V Boutou and J P Wolf, *Opt. Express* **15**, 13295 (2007)
[15] H T Wang, C Y Fan, H Shen, P F Zhang and C H Qiao, *Opt. Commun.* **293**, 113 (2013)
[16] S Tzortzakis, L Berge, A Couairon, M Franco, B Prade and A Mysyrowicz, *Phys. Rev. Lett.* **86(24)**, 5470 (2001)
[17] T P Todorov, M E Todorova, M D Todorov and I G Koprinkov, *Opt. Commun.* **323**, 128 (2014)
[18] J Bernhardt, W Liu, S L Chin and R Sauerbrey, *Appl. Phys. B* **91**, 45 (2008)
[19] S Eisenmann, J Penano, P Sprangle and A Zigler, *Phys. Rev. Lett.* **100**, 155003 (2008)
[20] H T Wang, C Y Fan, P F Zhang, C H Qiao, J H Zhang and H M Ma, *J. Opt. Soc. Am. B* **28(9)**, 2081 (2011)
[21] A Couairon, A Lotti, D Faccio, P D Trapani, D S Steingrube, E S Hulz, T Binhammer, U Morgner, M Kovacev and M B Gaarde, *Pramana – J. Phys.* **83(2)**, 221 (2014)
[22] P Béjot, J Kasparian, S Henin, V Loriot, T Vieillard, E Hertz, O Faucher, B Lavorel and J P Wolf, *Phys. Rev. Lett.* **104**, 103903 (2010)
[23] Z X Wang, C J Zhang, J S Liu, R X Li and Z Z Xu, *Opt. Lett.* **36(12)**, 2336 (2011)
[24] M Tarazkar, D A Romanov and R J Levis, *J. Chem. Phys.* **140**, 214316 (2014)
[25] P Béjot, J Kasparian and J P Wolf, *Opt. Express* **16**, 14115 (2008)
[26] G P Agrawal, *Nonlinear fiber optics*, 4th Edn (Academic, MA, 2013)
[27] W H Press, S A Teukolsky and W T Vetterling, *Numerical recipies*, 3rd Edn (William H. Press, Cambridge, 2007)
[28] A Chiron, B Lamouroux, R Lange, J F Ripoche, M Franco, B Prade, G Bonnaud, G Riazuelo and A Mysyrowicz, *Eur. Phys. J. D* **6**, 383 (1999)
[29] A Couairon and L Bergé, *Phys. Plasmas* **7(1)**, 193 (2000)
[30] J H Marburger, *Prog. Quant. Electron.* **43**, 5 (1975)
[31] E L Dawes and J H Marburger, *Phys. Rev.* **179(3)**, 862 (1969)